NDC80 kinetochore complex component is a potential molecular target of adenoid cystic carcinoma

XIA YAN[1*], SUMEI HE[2*], YUANSHENG LIN[3*], JIN ZHANG[4], JIAN HUAN[5], HAIBO CHEN[5] and LINA LU[5]

[1]Department of Oncology, Punan Branch of Renji Hospital, Shanghai Jiaotong University School of Medicine (Punan Hospital in Pudong), Shanghai 200125, P.R. China; [2]Department of Pharmacy, Suzhou Hospital, Affiliated Hospital of Medical School, Nanjing University, Suzhou, Jiangsu 215153, P.R. China; [3]Department of Emergency and Critical Care Medicine, Suzhou Hospital, Affiliated Hospital of Medical School, Nanjing University, Suzhou, Jiangsu 215153, P.R. China; [4]Department of Pathology, Suzhou Hospital, Affiliated Hospital of Medical School, Nanjing University, Suzhou, Jiangsu 215153, P.R. China; [5]Department of Radiation Oncology, Suzhou Hospital, Affiliated Hospital of Medical School, Nanjing University, Suzhou, Jiangsu 215153, P.R. China

Received June 14, 2025; Accepted November 25, 2025

DOI: 10.3892/ol.2026.15467

Abstract. Adenoid cystic carcinoma (ACC) is a slow-growing malignant tumour that primarily originates from the major and minor salivary glands. The relationship between the NDC80 kinetochore complex component (NUF2) and ACC remains to be elucidated. The present study obtained gene expression information from the Gene Expression Omnibus database (GSE88804 and GSE153002). Differentially expressed genes were identified by using the 'limma' package in R. A protein-protein interaction network was constructed with the Search Tool for Retrieval of Interacting Genes/Proteins database and key genes were extracted using Cytoscape software. Analysis of differential expression levels of hub genes in tumour and normal tissue was performed using Tumour Immune Estimation Resource (TIMER) and GSE36820 profiles. Gene Ontology enrichment was subsequently analysed based on differences in NUF2 expression in tumour tissues. In addition, single sample Gene Set Enrichment Analysis (ssGSEA) was used for the quantitative analysis of immune cell infiltration in ACC. Western blotting and immunohistochemistry were used to assess NUF2 expression levels in tumour and adjacent non-tumour tissues. Small interfering RNA (siRNA) was used to decrease NUF2 expression in ACC cell lines. The biological functions of NUF2 were analysed using Cell Counting Kit-8 and wound healing assays. A total of 248 differential genes were identified by differential expression analyses, with 113 genes upregulated and 135 downregulated. A total of 7 hub genes, namely, CDK1, budding uninhibited by benzimidazoles 1 mitotic checkpoint serine/threonine kinase B, DNA topoisomerase II α, cyclin B2, NUF2, budding uninhibited by benzimidazoles 1 and centromere protein F, were obtained using the 'cytoHubba' plugin. The TIMER, standardized and GSE36820 databases revealed that the expression levels of NUF2 were higher in ACC tissues compared with normal tissue samples. Western blotting and immunohistochemical staining of ACC tissues provided evidence of NUF2 upregulation in ACC tissue compared with normal tissue. NUF2-related genes were enriched in 'ameboidal-type cell migration', 'collagen-containing extracellular matrix' and 'actin binding'. ssGSEA analysis revealed that the expression level of NUF2 was notably associated with activated $CD4^+$ T cells, memory B cell and plasmacytoid dendritic cell. ACC cells transfected with NUF2 siRNA exhibited decreased proliferation and migration compared with the control. In conclusion, NUF2 is upregulated in ACC and is associated with immune cell infiltration. Functional studies demonstrated that NUF2 promotes ACC cell proliferation and migration, suggesting its potential as a therapeutic target for ACC.

Correspondence to: Dr Lina Lu, Department of Radiation Oncology, Suzhou Hospital, Affiliated Hospital of Medical School, Nanjing University, 1 Lijiang Road, Suzhou, Jiangsu 215153, P.R. China
E-mail: 18362722980@163.com

*Contributed equally

Key words: NDC80 kinetochore complex component, adenoid cystic carcinoma, differentially expressed gene, hub genes, immune cells

Introduction

Adenoid cystic carcinoma (ACC), also known as cylindroma, is a rare malignant tumour that accounts for 1% of all head and neck cancer (HNSC) and 10% of salivary gland malignancies (1). Salivary glands are the most common site of ACC, but tumours may also occur in the lacrimal glands (2), breast (3), nasal cavity and paranasal sinus (4) vulva (5) and skin (6). ACC occurring in the vulvar region predominantly arises from the Bartholin's gland. Although characterized by indolent growth, this malignancy commonly exhibits perineural invasion (7). The age of onset is between 18 and 90 years; however, no notable

differences have been identified between the sexes (8,9). At present, the common treatment is surgery with or without radiotherapy, as no approved systemic therapy exists. ACC of the head and neck progresses relatively slowly and indolently, resulting in 5- and 10-year patient survival rates of ~85 and 67%, respectively (8). However, long-term outcomes have revealed a decline in the 20-year overall survival rate of ~20% (10), which is primarily associated with nerve invasion, local control failure and distant metastasis (11). Due to the complexity of its clinical biological behaviour and the challenges in clinical treatment, ACC requires further investigation.

NDC80 kinetochore complex component (NUF2) is the gene encoding the protein cell division cycle associated 1, which serves a key role in ensuring proper chromosomal segregation and is a key component of the NDC80/NUF2 complex (12,13). Previous studies have reported that the expression level of the NUF2 gene increases in various cancer tissues and it is closely associated with tumorigenesis and progression, including hepatocellular carcinoma, clear cell renal cell carcinoma, gastric and breast cancer (13-17). It has been reported that in ovarian cancer, lung adenocarcinoma and breast cancer, downregulating the expression level of the NUF2 gene not only inhibits cell proliferation and colony formation, but also promotes apoptosis (18-20). These studies support the possible role of NUF2 in tumorigenesis.

Collectively, the high recurrence rate (50%) (21) and distant metastasis of ACC underscore the need for novel molecular targets. The established role of NUF2 in proliferation and migration positions it as a plausible contributor to ACC aggressiveness. However, to the best of our knowledge, no studies have investigated the function of NUF2 in ACC, leaving its therapeutic potential unexplored. Therefore, the aim of the present study was to screen the hub genes distinguishing ACC from normal tissues by the application of bioinformatics techniques. The present study identified the key role of NUF2 in ACC by analysing public datasets and further validated these findings using functional experiments.

Materials and methods

Patients and samples. ACC tissues and paired adjacent normal tissue samples were obtained from patients with ACC undergoing surgery at Suzhou Hospital, Affiliated Hospital of Medical School, Nanjing University (Suzhou, China) between October 2021 and December 2024 for immunohistochemistry (IHC) and western blotting analysis. The inclusion criteria were as follows: i) Age, 18-80 years; ii) postoperative pathological confirmation of adenoid cystic carcinoma; and iii) availability of complete clinical data. The exclusion criterion was a history of prior radiotherapy or chemotherapy. Due to the low incidence of ACC at Suzhou Hospital, Affiliated Hospital of Medical School, Nanjing University, only 2 patients met the inclusion criteria during the present study period. The present study was approved by the Ethics Committee of Suzhou Hospital, Affiliated Hospital of Medical School, Nanjing University (approval no. IRB2020094; Suzhou, China). Included patients signed a consent form that authorized the use of their tissues in the present study.

ACC dataset. In the present study, datasets were obtained from the GEO data repository (https://www.ncbi.nlm.nih.gov/geo/). The GSE88804 dataset contained 13 surgical samples of ACC with 7 normal samples (22). The GSE153002 dataset was composed of 30 ACC samples and 7 normal samples (23). The GSE36820 dataset included 11 ACC samples and 3 normal samples (https://www.ncbi.nlm.nih.gov/geo/query/acc.cgi?acc=GSE36820). The GSE88804 and GSE153002 datasets were merged and normalized utilizing the 'sva' R package (version no. 3.58.0; https://www.bioconductor.org/packages/release/bioc/html/sva.html; R Development Core Team; Bioconductor) and the normalized data were used for subsequent study. The GSE36820 dataset was utilized for verification.

Differentially expressed genes (DEGs). The R package 'limma' (version 3.58.1; https://bioinf.wehi.edu.au/limma/; R Development Core Team; Bioconductor) was used for the merged dataset. The fold-change (FC) was calculated using false discovery and the Benjamini-Hochberg method was used to adjust the original P-values (24). Based on adjusted $P<0.05$ and $\log_2FC >1$, the present study identified the DEGs in the merged dataset with the 'limma' package. Subsequently, a volcano plot and heatmap were generated to visualize the results.

Protein-protein interaction (PPI) network construction and hub gene exploration. The Search Tool for Retrieval of Interacting Genes/Proteins (STRING) database (https://cn.string-db.org/cgi/input?sessionId=bXmYsv7CnUrH&input_page_active_form=multiple_identifiers) displayed the relationships between proteins in the form of network graphs. In the present study, the DEGs were uploaded to the STRING website to construct a PPI network for the prediction of vital genes with a confidence score >0.4 and the organism was set to *Homo sapiens*. The network data were exported and imported to Cytoscape software (version 3.9.0) for analysis and visualization of the molecular interaction diagrams. Subsequently, 'cytoHubba', a plugin tool in Cytoscape (25), was used to separately identify the first hub genes based on three topological analysis methods, including degree, maximum clique centrality (MCC) and maximum network connectivity (MNC). The intersection of these genes were subsequently visualized.

Expression and validation analysis of NUF2. Tumour Immune Estimation Resource (TIMER) 2.0 is a database that utilizes RNA-sequencing (RNA-seq) expression profile data to analyse differential gene expression in tumours (http://timer.cistrome.org/). The differences in NUF2 expression between normal and cancer tissues in different cancer types were determined using the TIMER 2.0 database (26). In the present study, NUF2 was inputted into the 'Gene_DE' module (https://compbio.cn/timer2/) of the TIMER 2.0 database and the difference in NUF2 expression between normal and cancer tissues from different tumours in The Cancer Genome Atlas database was analysed (27).

The present study used box plots to depict the differential expression level of NUF2 in normal and tumour tissues using the combined dataset, after which the present study validated

the differential expression level of NUF2 in the GSE36820 dataset.

Functional enrichment analysis. Based on the median expression levels of NUF2 in tumour tissues, the two groups were divided into high- and low-expression groups and the differences were analysed using the 'limma' package. LogFC >1 and adjusted P<0.05 were set as the cut-off point for the DEGs. Gene Ontology (GO) enrichment analysis of the DEGs was performed with the 'ClusterProfiler' (version 4.10.0; https://yulab-smu.top/biomedical-knowledge-mining-book/) and 'org.Hs.eg.db' (version 3.22; https://bioconductor.org/packages/org.Hs.eg.db) package. Subsequently, the results were visualized using a bubble diagram.

Immune infiltration analysis. TIMER is a web server used to analyse the level of immune infiltration in different cancer types. In the TIMER database, specific algorithms were used to analyse the immune infiltration level. In the present study, the relationship between NUF2 and immune cells in HNSC was discussed.

To assess differences in immune cell infiltration, single sample Gene Set Enrichment Analysis (ssGSEA) was performed on RNA-seq data from the NUF2 high- and low-expression groups.

IHC. The tissue samples were fixed in 10% neutral formalin at room temperature for 24 h. IHC staining was performed on 4-μm-thick paraffin-embedded tissue sections. The sections were deparaffinized in xylene and rehydrated using a graded ethanol series to water. Antigen retrieval was carried out in citrate buffer (pH 6.0) at 121˚C for 120 sec using a pressure cooker. To quench endogenous peroxidase activity, the sections were incubated in 3% hydrogen peroxide solution protected from light for 25 min at room temperature. Non-specific binding sites were blocked with rabbit serum (concentrated; cat. no. G1209; Wuhan Servicebio Technology Co., Ltd.) for 30 min at room temperature. The sections were then incubated with primary antibody [rabbit polyclonal antibodies against NUF2 (1:500; cat. no. 15731-1-AP; Proteintech Group, Inc.)] overnight at 4˚C in a humidified chamber. Subsequently, the sections were incubated with HRP-conjugated goat anti-rabbit secondary antibody (1:200; cat. no. GB23303; Wuhan Servicebio Technology Co., Ltd.) at room temperature for 50 min. Colour development was performed using a DAB substrate kit according to the manufacturer's instructions (cat. no. G1212; Wuhan Servicebio Technology Co., Ltd.) at room temperature, followed by counterstaining with haematoxylin for ~3 min. Lastly, the stained sections were imaged under a light microscope. Each section was evaluated by two blinded, independent pathologists. Discrepancies between the two pathologists were resolved by a joint re-evaluation and discussion until a consensus was reached. The percentages of positive tumour cells were as follows: i) 1-25%; ii) 26-50%; iii) 51-75%; and iv) 76-100%. The immunoreaction intensity was classified as 0 (negative), 1 (weak), 2 (moderate), 3 (strong). The final staining scores were calculated as the sum of the intensity and positive rates scores and was graded as follows: 0 score, negative (-); 1-3 scores, weakly positive (+); 4-5 scores, moderate positive (++) or 6-7 scores, strongly positive (+++) (28).

Western blotting analysis. Proteins were isolated from human ACC tissues and paired adjacent normal tissues using RIPA buffer (Beyotime Institute of Biotechnology). The protein concentration was determined by the BCA method. Subsequently, 30 μg of protein was loaded onto an 10% SDS-PAGE gel and then transferred to PVDF membranes. The PVDF membranes were blocked with 5% milk at room temperature for 1 h and then incubated with the primary antibody against NUF2 (1:800; cat. no. 15731-1-AP; Proteintech Group, Inc.) and GAPDH (1:10,000; cat. no. 10494-1-AP; Proteintech Group, Inc.) overnight at 4˚C. After washing with TBS-0.1% Tween 20, the membranes were incubated with secondary antibodies (HRP-conjugated Goat Anti-Rabbit IgG; 1:5,000; cat. no. SA00001-2; Proteintech Group, Inc.) for 2 h at room temperature. Lastly, the bands were detected using an ECL substrate (Beyotime Institute of Biotechnology) according to the manufacturer's instructions and an Amersham™ Imager 680 system (Cytiva).

Cell culture. The human salivary ACC (SACC)-83 cell line (cat. No. FH0798; https://www.fudancell.com/sys-pd/?pid=3836) was purchased from Shanghai Fuheng Biotechnology Co., Ltd. The SACC-83 cell line was cultivated in RPMI 1640 medium (Gibco; Thermo Fisher Scientific, Inc.) supplemented with 1% penicillin/streptomycin and 10% FBS (cat. no. FH100-900; Shanghai Fuheng Biotechnology Co., Ltd) at 37˚C in a 5% CO_2 atmosphere.

Small interfering RNA (siRNA) and transfection. siRNAs targeting human the NUF2 gene and negative control siRNA (si-NC) were purchased from Guangzhou RiboBio Co., Ltd. SACC-83 cells were transfected with si-NC (cat. no. siN0000001-1-5) or siNUF2 (Table SI) using Lipofectamine® 3000 (Thermo Fisher Scientific, Inc.) according to the manufacturer's protocol. The cells were seeded into 6-well plates at a density of $2x10^5$ cells/well before transfection and cultured until they reached a confluency of 60-70%. Transfected cells were incubated at 37˚C for 72 h and then were collected for Cell Counting Kit-8 (CCK-8) assay and wound healing assay.

CCK-8. After 72 h target gene suppression, the cells were seeded in 96-well plates at a density of $1.5x10^3$ cells/well. A control group cultured with medium alone was established in parallel. At 24, 48, 72 and 96 h, 10 μl of CCK-8 solution (MedChemExpress) was added to each well under light-protected conditions. After a 2 h incubation, the absorbance at 450 nm was measured with a spectrophotometer (Tecan Biotechnology).

Wound healing assay. SACC-83 cells transfected with NUF2 siRNA were seeded in 6-well plates at a density of $1.5x10^5$ cells/well and cultured overnight to reach 80-90% confluence. Linear wounds were generated using a 1,000 μl pipette tip held orthogonal to the plate surface. After the cells were washed with post-scratch PBS, cellular debris was removed and 2 ml of serum-free RPMI-1640 was

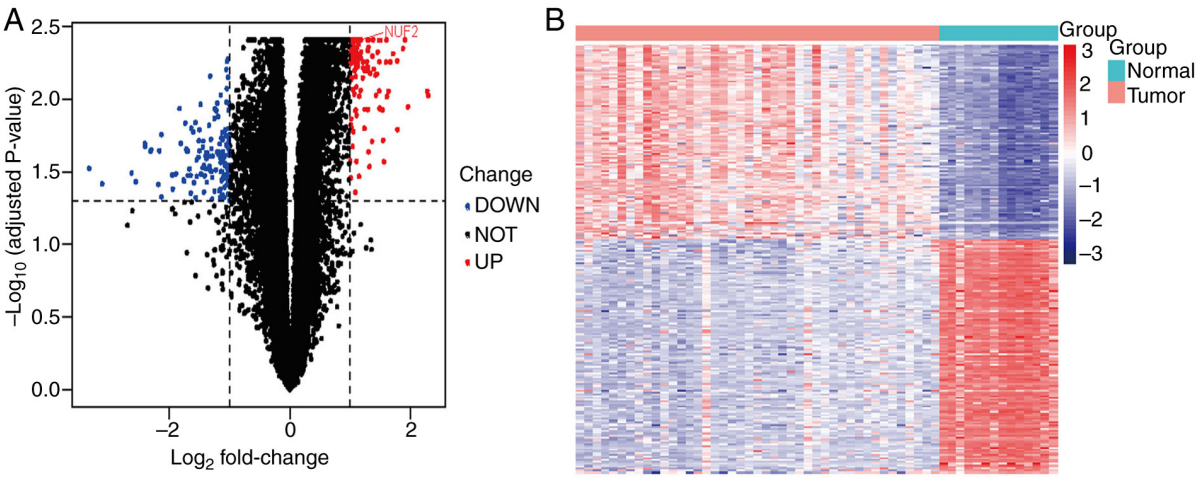

Figure 1. DEGs in GSE88804 and GSE153002. (A) Volcano map of DEGs (blue represents downregulated genes and red represents upregulated genes). (B) Heatmap of DEGs (blue represents down-regulated genes and red represents up-regulated genes). DEGs, differentially expressed genes; NUF2, NDC80 kinetochore complex component; GSE, Gene Set Enrichment.

added to mitigate the effects on proliferation. Cell migration was observed under an inverted microscope at 0 and 24 h post-culture. Quantification was conducted using ImageJ software. The wound area at 0 and 24 h was first measured, after which the wound closure rate was calculated. Wound closure was defined as the percentage reduction in wound area at 24 h relative to the initial wound area at 0 h. Each group included three independent biological replicates, and all data were presented as mean ± SD.

Statistical analysis. To evaluate immune infiltrates, TIMER 2.0 employs partial Spearman's correlation, controlling for tumour purity, to assess the association between the estimated levels of immune infiltration and NUF2 expression. Data obtained from the CCK-8 assay were analysed using one-way ANOVA, followed by the Bonferroni post-hoc test. The wound healing assay was analysed using an unpaired t-test. All statistical tests were two-tailed. CCK-8 and wound healing assay were performed in triplicate. The efficiency of NUF2 knockdown by each specific siRNA (si-1, si-2, and si-3) was evaluated via Western blot. Quantitative data were compared to the negative control group (si-NC) using one-way ANOVA, followed by the Bonferroni post-hoc test. Statistical analyses were performed with GraphPad Prism (version 10; Dotmatics). For comparisons between two groups of independent samples, such as tumour samples vs. normal control samples from different individuals in the GEO datasets, the Mann-Whitney U test was used. For comparisons involving paired samples with sufficient sample size (n≥5), the Wilcoxon signed-rank test was employed. $P<0.05$ was considered to indicate a statistically significant difference.

Results

Screening of DEGs. In the present study, three gene expression datasets, GSE88804, GSE153002 and GSE36820, were downloaded from the GEO database. A total of 54 ACC with 17 normal salivary gland tissues data were obtained. In the merged GSE88804 and GSE153002 datasets, the present study applied the rectified data for differential expression analysis and obtained 248 DEGs, including 113 upregulated genes and 135 downregulated genes (Fig. 1A and B).

PPI network and module analysis. To identify functionally pivotal interactions, an established DEG-associated PPI network was constructed using the STRING database and analysed using Cytoscape software. Based on network degree centrality analysis, the present study identified the top 10 hub genes with the highest connectivity for further investigation (Fig. 2A). Subsequently, the present study implemented the MCC and MNC algorithms to enhance the robustness of hub gene identification. The top 10 highest-scoring genes from each method were obtained (Fig. 2B and C). To identify key genes, the present study first selected the top 10 candidates from each method (degree, MCC and MNC) and then performed intersection analysis to identify seven high-confidence hub genes (CDK1, budding uninhibited by benzimidazoles 1 mitotic checkpoint serine/threonine kinase B, DNA topoisomerase II α, cyclin B2, NUF2, budding uninhibited by benzimidazoles 1 and centromere protein F; Fig. 2D). The role of NUF2 in ACC remains unexplored; a PubMed (https://pubmed.ncbi.nlm.nih.gov/) search using the keywords 'NUF2' and 'adenoid cystic carcinoma' yielded no relevant publications.

Expression and verification of NUF2. Analysis of the TIMER database using the 'Gene_DE' module demonstrated that NUF2 was significantly highly upregulated in a variety of tumours compared with normal tissues, such as liver hepatocellular carcinoma, oesophageal carcinoma, stomach adenocarcinoma, glioblastoma multiforme, breast invasive carcinoma and colon adenocarcinoma ($P<0.001$; Fig. 3A). In the combined and standardized datasets (GSE88804 and GSE153002), the expression levels of NUF2 were also significantly higher in tumour tissue samples compared with normal tissue samples ($P<0.001$; Fig. 3B). Similarly, NUF2 expression was significantly upregulated in ACC within the GSE36820 validation set ($P<0.01$; Fig. 3C). These results were also supported by western blotting analysis, which revealed a marked increase

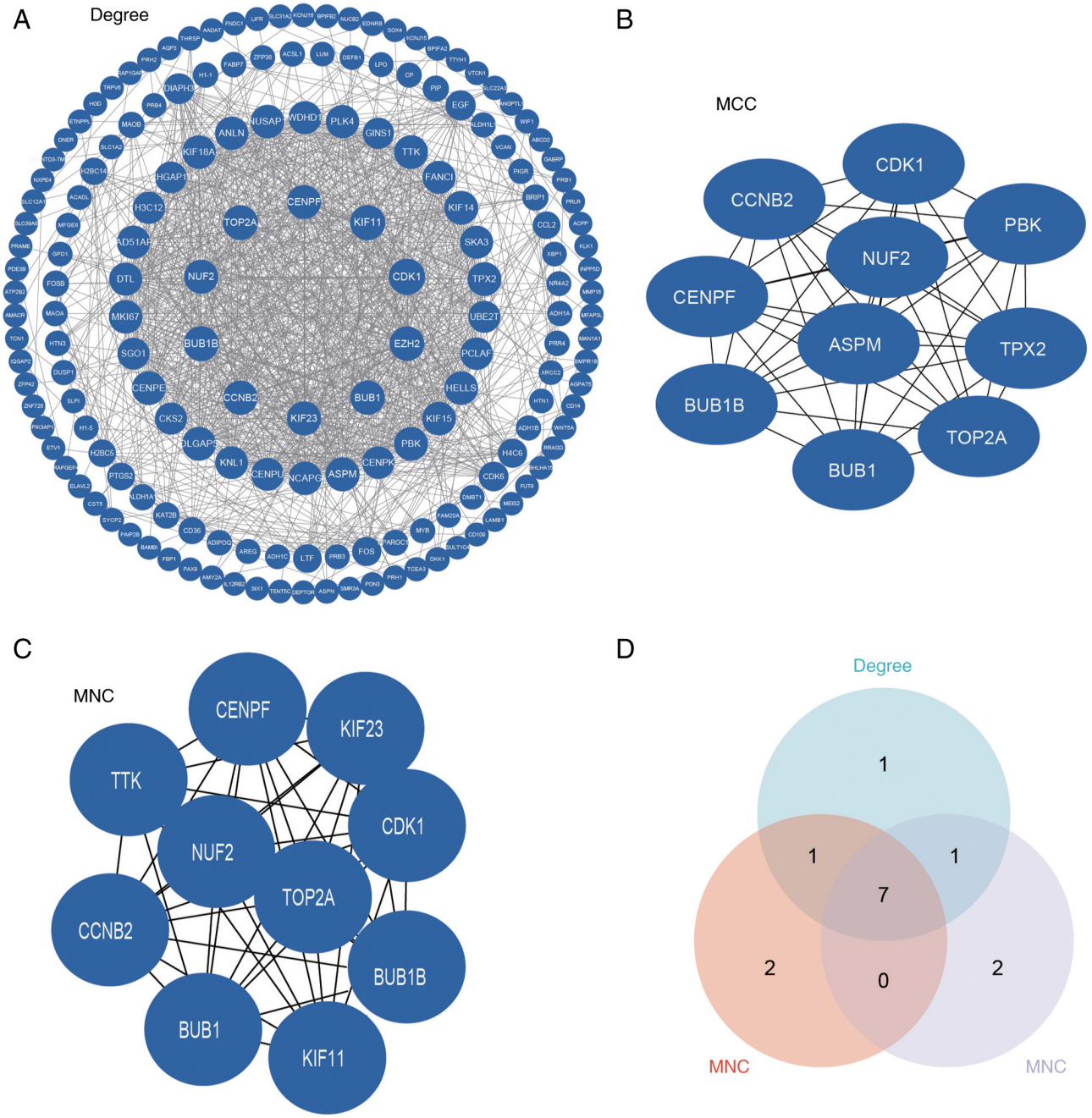

Figure 2. Construction and analysis of the PPI network. (A) PPI network of DEGs was constructed with Cytoscape. Degree was used to identify central genes. (B) MCC was used to identify central genes. (C) MNC was used to identify central genes. (D) Venn diagram was drawn and intersected. NUF2, NDC80 kinetochore complex component; MNC, maximum network connectivity; PPI, protein-protein interaction; DEGs, differentially expressed genes; MCC, maximum clique centrality.

in NUF2 protein levels in ACC tissues (Fig. 3D). IHC analysis of a preliminary set of paired samples (n=2) showed a trend of higher NUF2 expression in ACC tissues (IHC scores, 6 and 6) compared with their matched adjacent tissues (IHC scores, 3 and 4) (Fig. 3E).

GO enrichment analysis of DEGs. In the present study, NUF2-related genes were significantly enriched in 'ameboidal-type cell migration', 'chromosome segregation', 'nuclear division' ($P<0.01$) in biological processes and 'collagen-containing extracellular matrix' ($P<0.05$) in molecular functions and 'actin binding' ($P<0.05$) in cellular components (Fig. 4A-C), suggesting its potential role in ACC cell metastasis and proliferation.

Correlations between immune cells and the expression levels of NUF2 in ACC. To analyse the relationship between NUF2 expression and the state of tumour-infiltrating immune cells, the TIMER database was used to assess the association in HNSC tissues. The present study identified that NUF2 expression showed a significant but weak positive association with the infiltration levels of $CD4^+$ T cells ($\rho=0.296$; $P=2.08\times10^{-11}$), neutrophils ($\rho=0.183$; $P=4.59\times10^{-05}$). By contrast, NUF2 expression was negatively correlated with the infiltration of

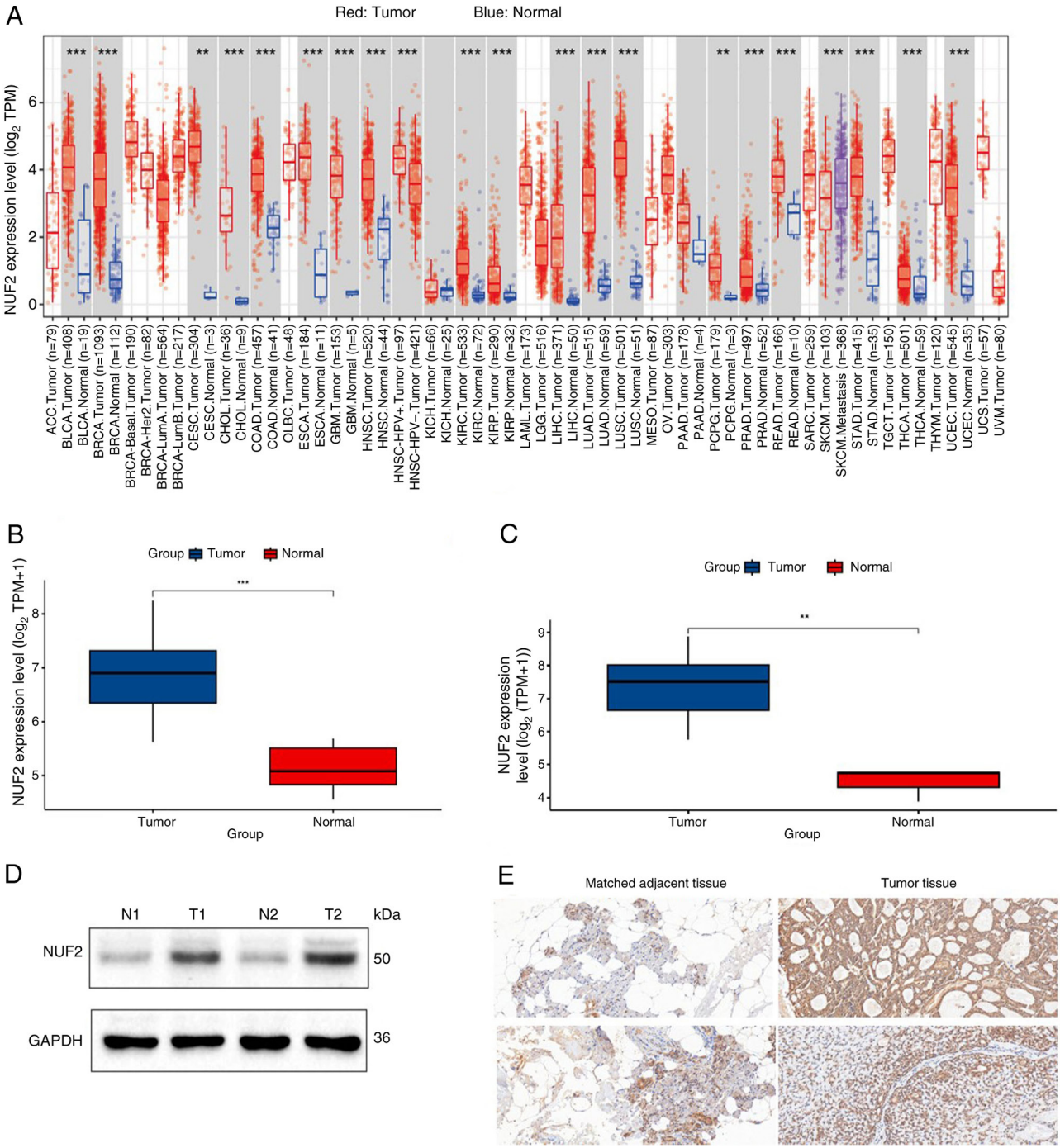

Figure 3. Expression level of NUF2 and immunohistochemistry. (A) Expression levels of NUF2 were analysed with the TIMER database. (B) Expression levels of NUF2 were verified with a merged dataset (GSE88804 and GSE153002). (C) Expression levels of NUF2 were verified by the GSE36820 dataset. (D) Expression levels of NUF2 in two ACC tissues and adjacent normal tissues assessed using western blotting. (E) Immunohistochemical staining results demonstrated that both tumour tissue samples received a final score of 6, indicating strong NUF2 expression. By contrast, the matched adjacent tissues demonstrated lower expression levels, with the upper adjacent tissue scoring 3 and the lower adjacent tissue scoring 4. Magnification, x200. **P<0.01 and ***P<0.001. siRNA, small interfering RNA; NUF2, NDC80 kinetochore complex component; TIMER, Tumour Immune Estimation Resource; GSE, Gene Set Enrichment; ACC, adenoid cystic carcinoma; TPM, transcripts per million; N, normal; T, tumour.

CD8$^+$ T cells (ρ=-0.372; P=1.29x10^{-17}) and B cells (ρ=-0.32; P=3.38x10^{-13}), with the correlation to CD8+ T cells being moderate. Only a very weak negative association was observed between NUF2 expression and macrophage infiltration (ρ=-0.104; P=2.08x10^{-02}; Fig. 5A).

Subsequently, ssGSEA was used to evaluate the infiltration of 28 immune cells in each patient with ACC. The results demonstrated that in the group with higher NUF2, activated CD4$^+$ T cells, γΔT cells, memory B cells and type 2 T helper cells were significantly more abundant in infiltration (P<0.05). The group with lower NUF2 expression demonstrated significantly increased infiltration (P<0.05) of activated dendritic cells, CD56 bright natural killer cells, central memory CD4$^+$ T cells, central memory CD8$^+$ T cells, immature dendritic cells, natural killer cells, natural killer T cells and plasmacytoid dendritic cells (Fig. 5B).

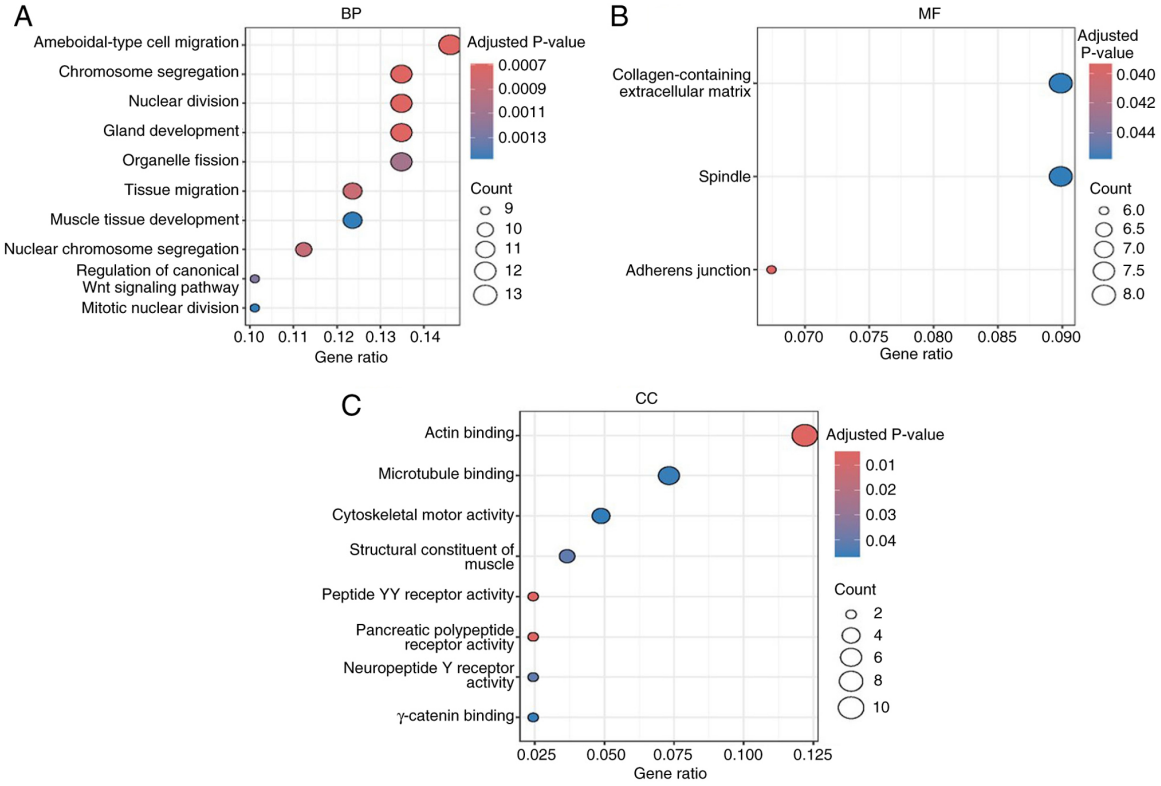

Figure 4. Functional enrichment analysis of NUF2-related genes. (A) Biological process of GO analysis. (B) Molecular functions of GO analysis. (C) Cellular components of GO analysis. siRNA, small interfering RNA; NUF2, NDC80 kinetochore complex component; GO, Gene Ontology.

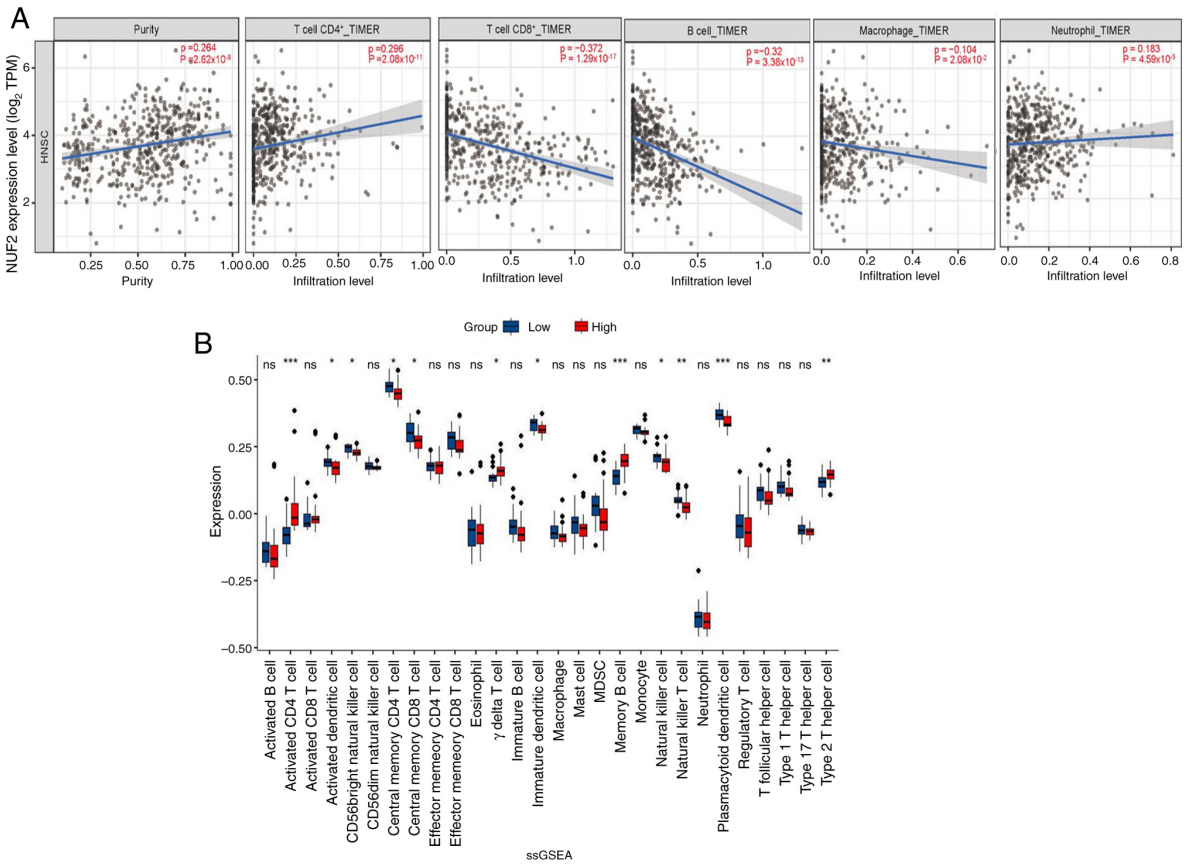

Figure 5. NUF2 expression correlates with the infiltration of immune cells. (A) Correlations between NUF2 expression and immune cells in HNSC tissues (n=522). (B) Box plots illustrating the degree of 28 immune infiltrating cell subtypes between the high- and low- NUF2 groups. *P<0.05, **P<0.01 and ***P<0.001. siRNA, small interfering RNA; NUF2, NDC80 kinetochore complex component; HNSC, head and neck cancer; ns, not significant; MDSC, myeloid-derived suppressor cells; TPM, transcripts per million; ssGSEA, single sample Gene Set Enrichment Analysis.

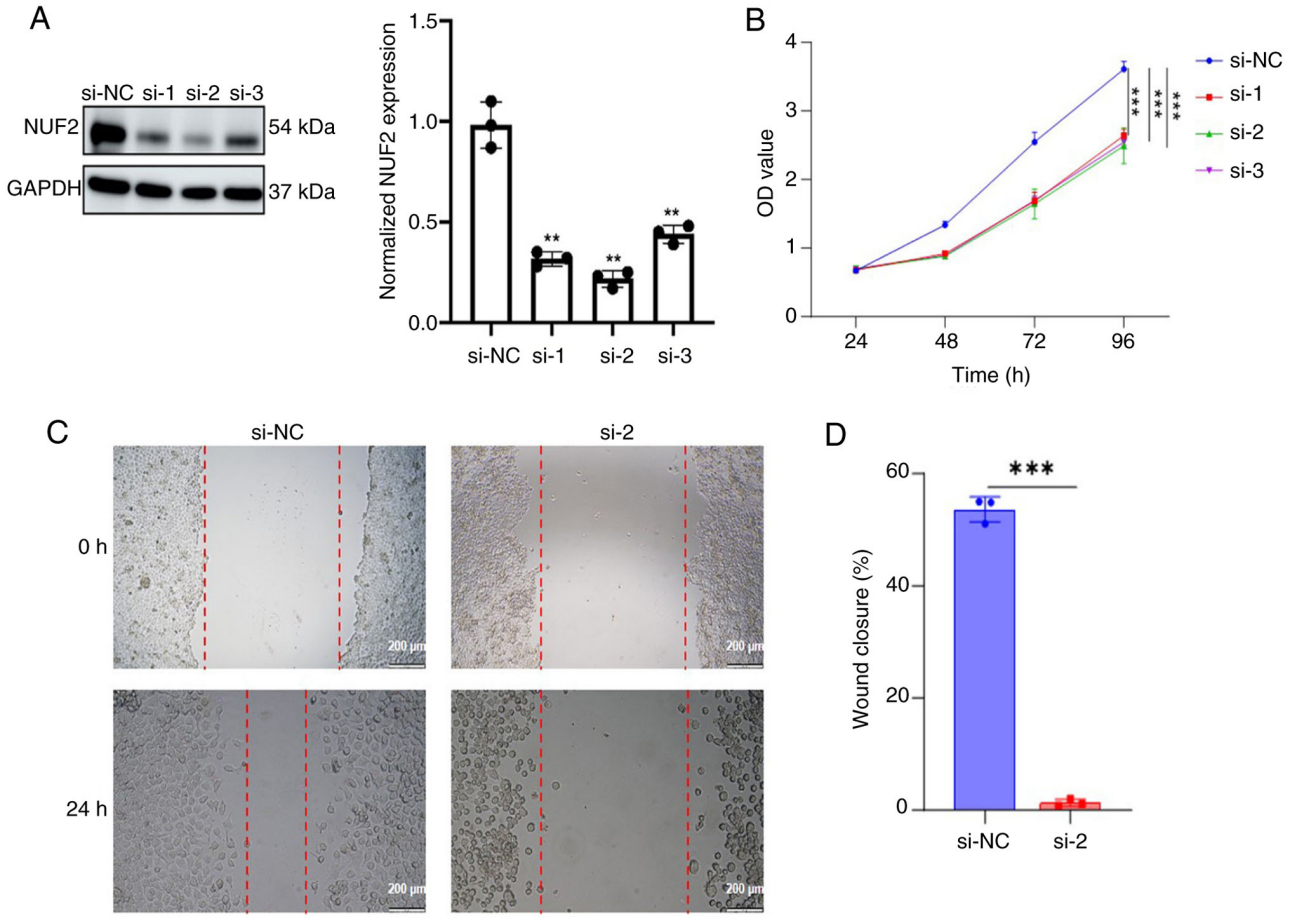

Figure 6. Knockdown efficiency of siNUF2 and NUF2 affects ACC proliferation and migration. (A) Western blotting analysis indicated the efficiency of NUF2 knockdown in SACC-83 cells transfected with si-NC and si-NUF2. (B) CCK-8 assay was used to assess the proliferation of the SACC-83 cells transfected with si-NC and si-NUF2. (C and D) Wound healing assay was performed to assess the migration of the SACC-83 cells transfected with si-NC and si-NUF2 and relative healing rate of SACC-83 after transfection. **P<0.01 and ***P<0.001. siRNA, small interfering RNA; NUF2, NDC80 kinetochore complex component; CCK-8, Cell Counting Kit-8; NC, negative control; ACC, adenoid cystic carcinoma; SACC, salivary ACC.

NUF2 promotes ACC cell proliferation and migration in vitro. To assess the biological effect of NUF2 in ACC cells, SACC-83 cells were transfected with siRNAs to silence NUF2 compared with the si-NC group. Western blotting was subsequently used to evaluate the transfection efficiency. The siRNA with the highest silencing efficiency, si-2, was selected for subsequent functional studies (Fig. 6A).

In the present study, a CCK-8 assay was performed in ACC cells. The downregulation of NUF2 expression significantly inhibited (P<0.0001) the proliferation of ACC cells (Fig. 6B). Subsequently, the present study explored the role of NUF2 in the migration of ACC cells using a wound healing assay. The results revealed that knockdown of NUF2 significantly diminished (P=0.0004) the migration capacity of ACC cells (Fig. 6C and D).

Discussion

As a result of the high risk of local recurrence and delayed distant metastases, the treatment outcomes for ACC remain suboptimal (29). Further research on the molecular mechanisms of ACC may offer potentially effective therapeutic strategies or promising biomarkers in the future. However, the sensitivity and specificity of these methods are limited. Increasing evidence suggests that NUF2 serves key roles in the development and progression of several tumours, such as ovarian cancer, multiple myeloma and hepatocellular carcinoma (20,30,31). However, the role of NUF2 in ACC remains to be elucidated and further research is warranted.

In the present study, the GEO database, western blotting and IHC analysis were used for gene expression analysis. The high expression level of NUF2 in tumour tissues and its low expression in normal tissues are consistent with previous findings (14,15,30). Furthermore, several studies have reported that NUF2 upregulation is associated with clinical stage and poor prognosis in adrenocortical cancer, kidney renal clear cell carcinoma, kidney renal papillary cell carcinoma and multiple myeloma (30,31). Fundamental research and clinical trials are needed to further validate NUF2 as a therapeutic target in ACC.

Several studies have reported that targeted regulation of NUF2 can inhibit cancer cell proliferation and migration. Liu *et al* (32) reported that silencing NUF2 expression could slow cell proliferation in human hepatocellular carcinomas. Furthermore, downregulation of NUF2 expression reduced the migratory ability of lung adenocarcinoma cells (18), which is consistent with the present study finding. In the present study, the GO analysis results revealed that NUF2 is potentially

involved in regulating both proliferation and migration processes in ACC.

Malignant tumours are composed of tumour cells, immune cells and non-immune cells. Immune and non-immune cells constitute the tumour microenvironment (TME), which includes components such as fibroblasts, nerves, immune cells and various cytokines and vascular systems (33). Increasing research has highlighted the key role of the TME in the genesis and progression of several malignancies such as laryngeal squamous cell carcinoma, brain metastasis (33-36) and liver cancer (37). Based on the status and distribution of immune cells, tumours are categorized into three immune phenotypes, including immune-desert ('cold' tumours), immune-exclusive and immune inflammatory ('hot' tumours) (38). 'Hot' tumours are characterized by abundant T-cell infiltration and exhibit good response to immune checkpoint inhibitors (39). Immunotherapy for numerous types of cancer has made notable progress. Immunotherapy is now a main therapeutic choice for advanced melanoma, renal cell carcinoma and renal cell carcinoma and is regarded as a promising method for cancer therapy (40-42). However, the expression levels of programmed death-ligand 1, cytotoxic T-cell antigen 4 and programmed death receptor 1 are low in the environment of ACC (43). Furthermore, several studies on the use of immunotherapy in ACC have reported unsatisfactory results (44,45). Li *et al* (46) identified that NUF2 is associated with the immune infiltration of certain immune cells, such as $CD8^+$ T Cells, B cells, natural killer cells and neutrophils. and has a major function in the regulation of cancer immunology. The present study results regarding the immune microenvironment suggested that elevated NUF2 expression in ACC is correlated with the infiltration of activated $CD4^+$ T cells, memory B cells and type 2 T helper cells. Further characterization indicated that high NUF2 expression was associated with increased infiltration of activated $CD4^+$ T cells, memory B cells and type 2 T helper cells, but decreased infiltration of plasmacytoid dendritic cells, activated dendritic cells and natural killer T cells. These findings suggest that the expression levels of NUF2 may influence the recruitment or activity of immune cells within the TME.

The present study had certain limitations. First, a notable limitation to consider is that HNSC and salivary gland cancer are distinct pathological entities. Consequently, extrapolating immune-related findings from this HNSCC cohort to ACC should be interpreted with caution. Second, the observed correlation between NUF2 expression and immune cell infiltration was inferred solely using *in silico* analysis using the ssGSEA algorithm. Immune correlations derived from bulk RNA-seq data can be susceptible to confounding factors such as tumour purity and stromal contamination (47). Additionally, the correlation analyses between NUF2 and immune cells derived from the TIMER database, particularly those involving $CD4^+$ T cells, neutrophils and macrophages, demonstrated weak associations, and their biological relevance remains to be determined. Third, the present study had a limited sample size. Therefore, to overcome these constraints, the collection of additional ACC specimens and the use of multiplex IHC coupled with flow cytometry in future studies may be used to validate the present study findings.

In summary, to the best of our knowledge, the present study provides the first analysis of the expression pattern of NUF2 in ACC. The present study results demonstrated that NUF2 is upregulated in ACC compared with that of adjacent tissues and NUF2 expression is correlated with immune cell infiltration. These findings may be potentially translated into effective clinical interventions in the future.

Acknowledgements

Not applicable.

Funding

No funding was received.

Availability of data and materials

The data generated in the present study may be requested from the corresponding author.

Authors' contributions

XY and LL conceived the present study and provided financial support. SH, YL, JZ, JH and HC performed the experiments, collected the data and prepared the figures. XY and LL confirm the authenticity of all the raw data. All authors read and approved the final version of the manuscript.

Ethics approval and consent to participate

The collection of tumour samples and patient information was approved by the Ethics Committee of Suzhou Hospital, Affiliated Hospital of Medical School, Nanjing University (approval no. IRB2020094; Suzhou, China). All patients signed informed consent for the retention and analysis of their tissues for research purposes.

Patient consent for publication

Not applicable.

Competing interests

The authors declare that they have no competing interests.

References

1. Coca-Pelaz A, Rodrigo JP, Bradley PJ, Vander Poorten V, Triantafyllou A, Hunt JL, Strojan P, Rinaldo A, Haigentz M Jr, Takes RP, *et al*: Adenoid cystic carcinoma of the head and neck-An update. Oral Oncol 51: 652-661, 2015.
2. Duarte AF, Alpuim Costa D, Cacador N, Boavida AM, Afonso AM, Vilares M and Devoto M: Adenoid cystic carcinoma of the palpebral lobe of the lacrimal gland-case report and literature review. Orbit 41: 605-610, 2022.
3. Gou WB, Yang YQ, Song BW and He P: Solid basal adenoid cystic carcinoma of the breast: A case report and literature review. Medicine (Baltimore) 103: e37010, 2024.
4. Lee TH, Kim K, Oh D, Yang K, Jeong HS, Chung MK and Ahn YC: Clinical outcomes in adenoid cystic carcinoma of the nasal cavity and paranasal sinus: A comparative analysis of treatment modalities. Cancers (Basel) 16: 1235, 2024.

5. Gural Z, Yucel S and Agaoglu F: Bartholin's gland adenoid cystic carcinoma: Report of three cases and the review of literature. Indian J Cancer 61: 346-349, 2024.
6. Schembri-Wismayer D, Gupta S and Erickson LA: Cutaneous adenoid cystic carcinoma. Mayo Clin Proc 99: 1017-1018, 2024.
7. Baker GM, Selim MA and Hoang MP: Vulvar adnexal lesions: A 32-year, single-institution review from Massachusetts General Hospital. Arch Pathol Lab Med 137: 1237-1246, 2013.
8. Atallah S, Casiraghi O, Fakhry N, Wassef M, Uro-Coste E, Espitalier F, Sudaka A, Kaminsky MC, Dakpe S, Digue L, *et al*: A prospective multicentre REFCOR study of 470 cases of head and neck Adenoid cystic carcinoma: Epidemiology and prognostic factors. Eur J Cancer 130: 241-249, 2020.
9. de Morais EF, da Silva LP, Moreira DGL, Mafra RP, Rolim LSA, de Moura Santos E, de Souza LB and de Almeida Freitas R: Prognostic factors and survival in adenoid cystic carcinoma of the head and neck: A retrospective clinical and histopathological analysis of patients seen at a cancer center. Head Neck Pathol 15: 416-424, 2021.
10. Dodd RL and Slevin NJ: Salivary gland adenoid cystic carcinoma: A review of chemotherapy and molecular therapies. Oral Oncol 42: 759-769, 2006.
11. Ellington CL, Goodman M, Kono SA, Grist W, Wadsworth T, Chen AY, Owonikoko T, Ramalingam S, Shin DM, Khuri FR, *et al*: Adenoid cystic carcinoma of the head and neck: Incidence and survival trends based on 1973-2007 surveillance, epidemiology, and end results data. Cancer 118: 4444-4451, 2012.
12. Nabetani A, Koujin T, Tsutsumi C, Haraguchi T and Hiraoka Y: A conserved protein, Nuf2, is implicated in connecting the centromere to the spindle during chromosome segregation: A link between the kinetochore function and the spindle checkpoint. Chromosoma 110: 322-334, 2001.
13. Xie X, Jiang S and Li X: Nuf2 is a prognostic-related biomarker and correlated with immune infiltrates in hepatocellular carcinoma. Front Oncol 11: 621373, 2021.
14. Liu Y, Wang Y, Wang J, Jiang W, Chen Y, Shan J, Li X and Wu X: NUF2 regulated the progression of hepatocellular carcinoma through modulating the PI3K/AKT pathway via stabilizing ERBB3. Transl Oncol 44: 101933, 2024.
15. Zheng B, Wang S, Yuan X, Zhang J, Shen Z and Ge C: NUF2 is correlated with a poor prognosis and immune infiltration in clear cell renal cell carcinoma. BMC Urol 23: 82, 2023.
16. Zhu X, Zou Y, Wu T, Ni J, Tan Q, Wang Q and Zhang M: ANP32E contributes to gastric cancer progression via NUF2 upregulation. Mol Med Rep 26: 275, 2022.
17. Zhai X, Yang Z, Liu X, Dong Z and Zhou D: Identification of NUF2 and FAM83D as potential biomarkers in triple-negative breast cancer. PeerJ 8: e9975, 2020.
18. Jiang F, Huang X, Yang X, Zhou H and Wang Y: NUF2 expression promotes lung adenocarcinoma progression and is associated with poor prognosis. Front Oncol 12: 795971, 2022.
19. Lv S, Xu W, Zhang Y, Zhang J and Dong X: NUF2 as an anticancer therapeutic target and prognostic factor in breast cancer. Int J Oncol 57: 1358-1367, 2020.
20. Ren M, Zhao H, Gao Y, Chen Q, Zhao X and Yue W: NUF2 promotes tumorigenesis by interacting with HNRNPA2B1 via PI3K/AKT/mTOR pathway in ovarian cancer. J Ovarian Res 16: 17, 2023.
21. Yuce Sari S, Yazici G, Elmali A, Bayatfard P, Koc I, Kiratli H and Cengiz M: Radiotherapy for adenoid cystic carcinoma of the lacrimal gland: Study on twelve patients. Cancer Radiother 29: 104644, 2025.
22. Andersson MK, Afshari MK, Andren Y, Wick MJ and Stenman G: Targeting the oncogenic transcriptional regulator MYB in adenoid cystic carcinoma by inhibition of IGF1R/AKT signaling. J Natl Cancer Inst 109: djx017, 2017.
23. Persson M, Andersson MK, Sahlin PE, Mitani Y, Brandwein-Weber MS, Frierson HF Jr, Moskaluk C, Fonseca I, Ferrarotto R, Boecker W, *et al*: Comprehensive molecular characterization of adenoid cystic carcinoma reveals tumor suppressors as novel drivers and prognostic biomarkers. J Pathol 261: 256-268, 2023.
24. Hochberg Y and Hochberg Y: Controlling the false discovery rate a practical and powerful approach to multiple testing. J Royal Stat Soc Series B 57: 289-300, 1995.
25. Chin CH, Chen SH, Wu HH, Ho CW, Ko MT and Lin CY: cytoHubba: Identifying hub objects and sub-networks from complex interactome. BMC Syst Biol 8 (Suppl 4): S11, 2014.
26. Li T, Fu J, Zeng Z, Cohen D, Li J, Chen Q, Li B and Liu XS: TIMER2.0 for analysis of tumor-infiltrating immune cells. Nucleic Acids Res 48: W509-W514, 2020.
27. Hutter C and Zenklusen JC: The cancer genome atlas: Creating lasting value beyond its data. Cell 173: 283-285, 2018.
28. Lin J, Chen X, Yu H, Min S, Chen Y, Li Z and Xie X: NUF2 drives clear cell renal cell carcinoma by activating HMGA2 transcription through KDM2A-mediated H3K36me2 demethylation. Int J Biol Sci 18: 3621-3635, 2022.
29. Stawarz K, Durzynska M, Galazka A, Gorzelnik A, Zwolinski J, Paszkowska M, Bieńkowska-Pluta K and Misiak-Galazka M: Current landscape and future directions of therapeutic approaches for adenoid cystic carcinoma of the salivary glands (Review). Oncol Lett 29: 153, 2025.
30. Wang Y, Chen L, Luo Y, Shen J and Zhou S: Predictive value of NUF2 for prognosis and immunotherapy responses in pan-cancer. Nan Fang Yi Ke Da Xue Xue Bao 45: 137-149, 2025 (In Chinese).
31. Zhang S, Zhang L, Cai L, Chen H, Wang Y, Yuan Y, Zhang H and Wei X: NUF2 overexpression predicts poor outcomes in multiple myeloma. Genes Dis 12: 101268, 2025.
32. Liu Q, Dai SJ, Li H, Dong L and Peng YP: Silencing of NUF2 inhibits tumor growth and induces apoptosis in human hepatocellular carcinomas. Asian Pac J Cancer Prev 15: 8623-8629, 2014.
33. Elhanani O, Ben-Uri R and Keren L: Spatial profiling technologies illuminate the tumor microenvironment. Cancer Cell 41: 404-420, 2023.
34. Binnewies M, Roberts EW, Kersten K, Chan V, Fearon DF, Merad M, Coussens LM, Gabrilovich DI, Ostrand-Rosenberg S, Hedrick CC, *et al*: Understanding the tumor immune microenvironment (TIME) for effective therapy. Nat Med 24: 541-550, 2018.
35. Rodrigo JP, Sanchez-Canteli M, Lopez F, Wolf GT, Hernández-Prera JC, Williams MD, Willems SM, Franchi A, Coca-Pelaz A and Ferlito A: Tumor-infiltrating lymphocytes in the tumor microenvironment of laryngeal squamous cell carcinoma: Systematic review and meta-analysis. Biomedicines 9: 486, 2021.
36. de Visser KE and Joyce JA: The evolving tumor microenvironment: From cancer initiation to metastatic outgrowth. Cancer Cell 41: 374-403, 2023.
37. Affo S, Yu LX and Schwabe RF: The role of cancer-associated fibroblasts and fibrosis in liver cancer. Annu Rev Pathol 12: 153-186, 2017.
38. Chen DS and Mellman I: Elements of cancer immunity and the cancer-immune set point. Nature 541: 321-330, 2017.
39. Xu Q, Hu J, Wang Y and Wang Z: The role of tumor types in immune-related adverse events. Clin Transl Oncol 27: 3247-3260, 2025.
40. Garg P, Pareek S, Kulkarni P, Horne D, Salgia R and Singhal SS: Next-Generation immunotherapy: Advancing clinical applications in cancer treatment. J Clin Med 13: 6537, 2024.
41. Liu B, Zhou H, Tan L, Siu KTH and Guan XY: Exploring treatment options in cancer: Tumor treatment strategies. Signal Transduct Target Ther 9: 175, 2024.
42. Waldman AD, Fritz JM and Lenardo MJ: A guide to cancer immunotherapy: From T cell basic science to clinical practice. Nat Rev Immunol 20: 651-668, 2020.
43. Wolkow N, Jakobiec FA, Afrogheh AH, Kidd M, Eagle RC, Pai SI and Faquin WC: PD-L1 and PD-L2 expression levels are low in primary and secondary adenoid cystic carcinomas of the orbit: Therapeutic implications. Ophthalmic Plast Reconstr Surg 36: 444-450, 2020.
44. Mosconi C, de Arruda JAA, de Farias ACR, Oliveira GAQ, de Paula HM, Fonseca FP, Mesquita RA, Silva TA, Mendonça EF and Batista AC: Immune microenvironment and evasion mechanisms in adenoid cystic carcinomas of salivary glands. Oral Oncol 88: 95-101, 2019.
45. Sato R, Yamaki H, Komatsuda H, Wakisaka R, Inoue T, Kumai T and Takahara M: Exploring immunological effects and novel immune adjuvants in immunotherapy for salivary gland cancers. Cancers (Basel) 16: 1205, 2024.
46. Li X, Zhang L, Yi Z, Zhou J, Song W, Zhao P, Wu J, Song J and Ni Q: NUF2 is a potential immunological and prognostic marker for non-small-cell lung cancer. J Immunol Res 2022: 1161931, 2022.
47. Yoshihara K, Shahmoradgoli M, Martinez E, Vegesna R, Kim H, Torres-Garcia W, Treviño V, Shen H, Laird PW, Levine DA, *et al*: Inferring tumour purity and stromal and immune cell admixture from expression data. Nat Commun 4: 2612, 2013.